Phenotypically Selected Mutations in Myosin's Actin Binding Domain Demonstrate Intermolecular Contacts Important for Motor Function†

Kim C. Giese and James A. Spudich*

Departments of Biochemistry and Developmental Biology, Stanford University School of Medicine, Stanford, California 94305

Received December 23, 1996; Revised Manuscript Received April 2, 1997⊗

ABSTRACT: Here, we biochemically characterize *Dictyostelium* myosin II mutants that were previously phenotypically selected following random mutagenesis and shown to lie in the actin binding domain [Patterson, B., & Spudich, J. A. (1996) *Genetics 143*, 801−810]. We show that the conditional loss of myosin-dependent activity in vivo, which results from the mutations E531Q, P536R, and R562L, is likely due to the loss of important contacts with actin. Purified wild-type and mutant myosin subfragments 1 (S1), expressed in *Dictyostelium*, are alike in binding to actin and releasing it in an ATP-dependent manner. Furthermore, the rates of ATP hydrolysis without actin are similar for the mutant and wild-type S1s. Thus, the mutations in the actin binding site have little effect on ATP binding or product release in the absence of actin. All three mutants, however, have impaired actin-activated ATPase activity, with apparent second-order rate constants for actin interactions that are 4−25-fold smaller than that of wild-type S1 at 30 °C. The mutations also cause defects in the ability to move actin, as measured by in vitro motility assays of full-length myosins. On the basis of motility of a mixture of wild-type and mutant myosins, there appears to be at least two classes of mutations, with the primary defect in either a weak or a strong actin binding state. In summary, the activities in vitro of myosins with mutations in the actin binding site suggest losses of important contacts with actin.

Directed movement and force production between myosin and actin filaments, whether in muscle fibers or nonmuscle cells, are dependent on changing interactions between the two proteins at specific points in myosin's ATPase cycle. As shown in Scheme 1, based on the work of Lymn and Taylor (1971) and many others in the field, the associations between myosin (M) and actin (A) are regulated by the nucleotide bound to myosin. A strong "rigor" interaction that occurs in the absence of nucleotide is disrupted when myosin binds ATP. While bound to ATP or the products of its hydrolysis, ADP and inorganic phosphate (P_i),[1] myosin is in rapid equilibrium between the weakly actin-bound and actin-free forms. The weak association with actin stimulates P_i release, and this release is coupled to a transition from weak to strong actin binding. The force-generating step occurs rapidly after this transition, but myosin remains tightly bound to actin until ADP is released and another ATP is bound [for reviews, see Huxley (1969), Goldman (1987), and Geeves (1991)]. These changing interactions allow myosin to generate a brief positive force and then to release actin so that the myosin is not creating a drag force on actin during the rest of the cycle. Furthermore, the coupling of P_i release to actin binding helps ensure that the energy of ATP hydrolysis is used in a productive manner. Thus, the interactions between actin and myosin are dynamic and

Scheme 1

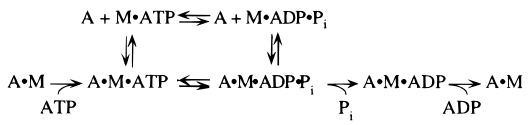

complex during the ATPase cycle. The challenge remains to understand what these interactions are, as well as how they change during force generation.

Of the actin−myosin binding states, rigor is best characterized due to its stability. Chemical cross-linking studies and docking of the structures of the motor domain, myosin subfragment-1 (S1) (Rayment et al., 1993b), with a model of filamentous actin based on the actin monomer crystal structure (Holmes et al., 1990) agree that in the rigor state myosin can bind two adjacent actin monomers (Yamamoto, 1990; Rayment et al., 1993a; Schröder et al., 1993). The docking suggests that there are numerous potential hydrophobic and ionic interactions that are likely to occur, although the exact contacts will depend on the conformational changes that occur as myosin binds actin. The actin−myosin weakly bound state that can occur when ATP or ADP•P_i is bound to myosin is based on ionic interactions and can be shielded by moderate salt concentrations. Myosin's lysine-rich 50/20 kDa loop in the actin binding region has been shown to be important for this weak interaction, as cleavage at certain sites in this loop lower the actin-activated ATPase of S1 due to reduced affinity for actin (Yamamoto, 1991).

The strong interaction between actin and myosin during force production is transient at physiological ATP concentrations (over in a few milliseconds) and may or may not change during the stroke. Huxley and Simmons (1971) proposed that there may be a rolling interaction, in which new bonds are formed as others are broken, and that this interaction

† This work was supported by Grant GM33289 to J.A.S. from the NIH. K.C.G. was supported by training Grant 5T32 GM07276-22 from the NIH.

* To whom correspondence should be addressed at the Department of Biochemistry, SUMC, Stanford, CA 94305. Phone: (415) 723-7634. Fax: (415) 725-6044. E-mail: jspudich@cmgm.stanford.edu.

⊗ Abstract published in *Advance ACS Abstracts,* June 1, 1997.

[1] Abbreviations: S1, subfragment 1; P_i, inorganic phosphate; kb, kilobase; DTT, dithiothreitol; PMSF, phenylmethanesulfonyl fluoride; TLCK, *N*α-*p*-tosyl-L-lysine chloromethyl ketone; PAGE, polyacrylamide gel electrophoresis; BSA, bovine serum albumin.

S0006-2960(96)03141-8 CCC: $14.00

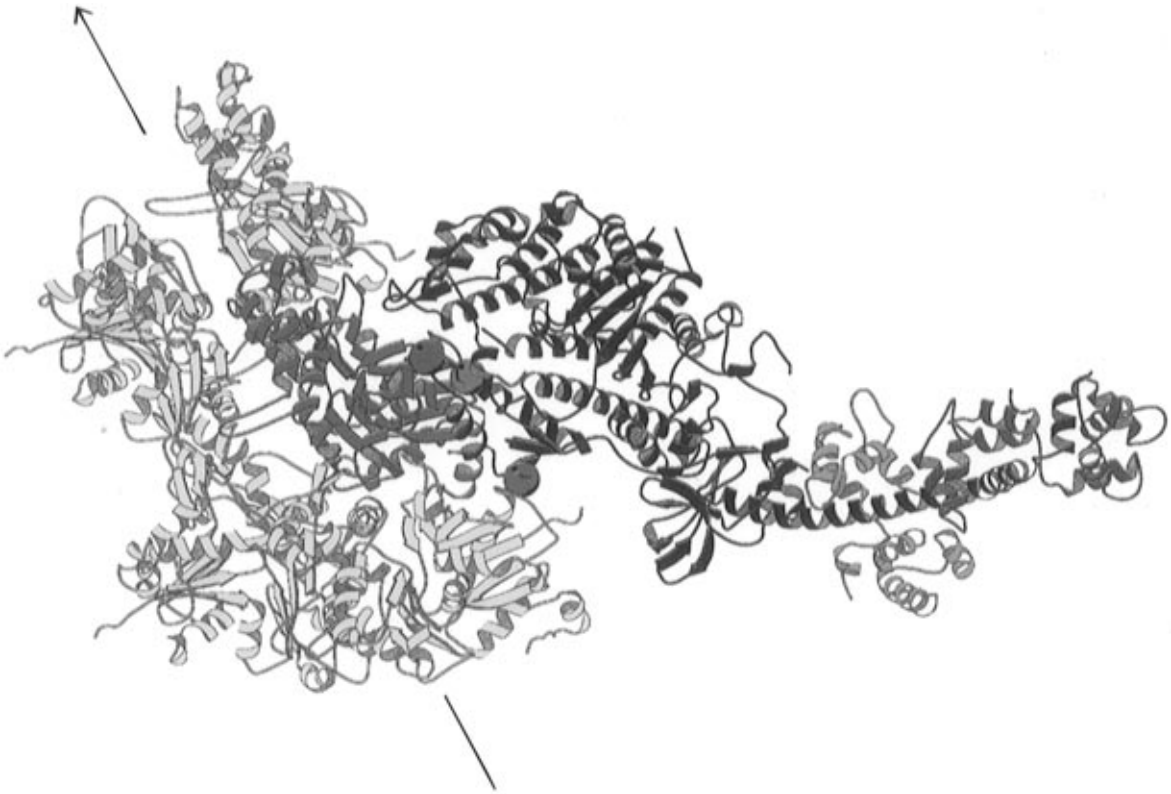

FIGURE 1: Potential contacts based on docking of S1 and actin filament structures. The crystal structure of chicken skeletal myosin (Rayment et al., 1993b) is shown docked to a model of an actin filament (Schröder et al., 1993). One actin monomer (referred to as the "first actin" in the text) is shown in red, and four other actin monomers are shown in yellow. The line shows the orientation of the actin filament, with the arrow head indicating the pointed end of the filament. The myosin heavy chain is in blue, the myosin essential and regulatory light chains are shown in orange and purple, respectively. The spheres show the alpha carbon positions of the chicken myosin residues E538 (cyan), P543 (green), and K569 (magenta), which correspond to the mutated *Dictyostelium* residues E531Q, P536R, and R562L. The figure was prepared using the structure program MOLSCRIPT (Kraulis, 1991).

may in part be responsible for force production. Another possibility is that force generation is due entirely to a conformational change of the head distal to actin, specifically the light chain binding region (Whittaker et al., 1995; Uyeda et al., 1996), and there is no motion at the actin−myosin interface during force production. If this were so, we would predict that the loss of specific contacts between actin and myosin may affect actin binding and/or release, but not myosin's force-generating stroke.

Complementing the structural predictions, information about the interactions that occur between actin and myosin throughout the cycle has come from molecular genetic studies. For example, chimeric myosins with different sequences at the highly variable region of the head known as the 50/20 kDa loop were shown to increase myosin's actin-activated ATPase activity, without increasing the rates at which they move actin (Uyeda et al., 1994). The changes in ATPase activity with such chimeras has been demonstrated to be due to changes in the apparent weak-binding affinity to actin, or K_m for actin, with little effect on V_{max} (Rovner et al., 1995). Mutations at the negatively charged amino terminus of actin have shown that this region affects both myosin's affinity for actin and the V_{max} of the actin-activated myosin ATPase activity (Sutoh et al., 1991; Cook et al., 1993). Such studies allow the correlation of structural sites to biochemical functions. With the exception of the myosin loop chimeras, most of the mutagenesis has been done on actin [for example, Johara et al. (1993) and Miller and Reisler (1995)]. The only single point mutation in myosin's actin binding site that has been studied biochemically was made based on a mutation, R403Q, that causes familial hypertrophic cardiomyopathy. This mutant was shown to have decreased actin activation of its ATPase rate (V_{max} was decreased and K_m for actin was increased by at least 3-fold each) and impaired activity in an in vitro motility assay (Sweeney et al., 1994). Further work is needed for us to fully understand the role of specific interactions between actin and myosin in force generation.

We describe here a study of mutants of *Dictyostelium discoideum* myosin II that are located in the actin binding site. These were isolated by Patterson and Spudich (1995) on the basis that cells expressing these myosin mutants have very low myosin function at nonpermissive temperatures, but retain some function at higher temperatures. The mutations, E531Q, P536R, and R562L (which correspond to the chicken skeletal myosin residues E538, P543, and K569, respectively), are located on the surface of the molecule in the actin binding domain as shown in Figure 1 (Patterson & Spudich, 1996). As cold-sensitive mutants, they have defects that do not abolish function, but rather limit it at the low temperature in vivo. On the basis of their location, we hypothesized that these mutations under nonpermissive conditions may cause a failure of myosin to properly bind or release actin at distinct intermediate stages of the ATPase cycle, and in this way obstruct myosin function.

We can guess at the nature of the contacts involved in particular mutations, based on the changes in charge or hydrophobicity. However, partners for and the functions of these contacts are more difficult to predict. The docking of the crystal structures places E531Q and P536R against the "first actin" monomer (Rayment et al., 1993a; Schröder et al., 1993) in a hydrophobic region that has been shown to

be important for rigor binding as well as actin activation (Miller et al., 1996). The R562L mutation lies in the region that was docked against the "second actin" monomer in a region that contains the charged pair E99/E100 (Rayment et al., 1993a). This pair has been shown to be important for weak binding to myosin and to have little effect on myosin's ability to move the E99A/E100A actin if the actin filaments are prevented from diffusing away (Miller & Reisler, 1995). The complementary charges of these actin and myosin residues suggest a possible interaction of R562 [whose positive charge is conserved in many myosins (Sellers & Goodson, 1995)] with the actin pair E99/E100. If this is the case, we expect the loss of charge on the myosin to have similar effects as the loss of charge on actin.

Such mutants can demonstrate the importance of a particular residue in one or more types of actin binding. Understanding the defects of these mutations on a biochemical level will help us define the number and nature of actin binding sites and the changes in binding interactions that occur as part of myosin's stroke.

MATERIALS AND METHODS

Plasmid Construction. All subcloning was done using standard procedures (Sambrook et al., 1989). Versions of pLittle·S1-His_6* (where * represents any of the three mutations) containing the point mutations E531Q, P536R, or R562L were created as follows. A purified 1 kb *Bgl*II/*Sac*I fragment from pTIKL·S1-His (Uyeda, T. Q.-P., unpublished data) was subcloned into the plasmids pLittle·myo* each containing one of the point mutations (Patterson & Spudich, 1995) at the *Bgl*II and *Sac*I sites. This deleted roughly 2/3 of the myosin gene C-terminal to the point mutations as well as terminator sequence and replaced them with the equivalent myosin coding sequence up to V865 followed by Pro-His-His-His-His-His-His-stop and a region of MyD 3′ flanking DNA. This creates a fragment equivalent to the myosin head fragment (Manstein et al., 1989a) with a 6× histidine tag. Later experiments were done using plasmids based on pTIKL·OE·S1, which carries copies of both myosin light chain genes (the regulatory light chain gene is fused to a six histidine repeat), as well as the truncated heavy chain (Uyeda, T. Q. P., unpublished data). This was used to make versions of pTIKL·OE·S1-His_6* by replacing the *Eco*NI/*Bst*XI fragment with equivalent fragments from pLittle·S1-His_6*. The presence of the mutations were verified by determining that a second *Xho*I site (due to a silent change in the original pLittle·myo*) had been introduced.

Dictyostelium Manipulations. All cells were grown in HL-5 (Sussman, 1987) with 17% FM Medium (Gibco BRL), 100 units/mL penicillin, 100 μg/mL streptomycin on petri dishes at 22 °C. Plasmids were electroporated into HS1, a myosin II null (*mhcA*-) strain derived from JH10 (Ruppel et al., 1994) by standard procedures (Egelhoff et al., 1991). Transformants were selected for and maintained with 5 μg/mL G418 (Gibco BRL).

Protein Purification. S1-His_6 proteins were purified according to the procedure of Manstein and Hunt (1995) with the some modifications. Cells were harvested from 530 cm^2 petri dishes (Nunc) by scraping. These were washed once and then resuspended in 3 mL of lysis buffer per gram of cells (wet weight). This was frozen dropwise in liquid nitrogen and stored at −80 °C. Lysis occurred when the cells, typically 50 g per preparation, were thawed with an additional 3 mL lysis buffer per gram of cells. The lysate was depleted of ATP, and the actin-bound S1 was pelleted, washed once, and then extracted with Mg^{2+}ATP. The resulting supernatant was loaded onto a Ni^{2+}-affinity column (Ni-NTA, Qiagen Inc.) and washed first with 300 mM sodium acetate and then 30 mM imidazole. Elution of S1-His_6 was achieved with a 30−300 mM gradient of imidazole, and the protein typically eluted near 100 mM imidazole. Samples were analyzed on 15% SDS−PAGE. Pooled fractions were dialyzed briefly against 60% sucrose to concentrate the sample and then overnight against 10 mM HEPES, pH 7.4, 0.5 mM EDTA, 1 mM DTT, 40 μg/mL TLCK, 0.1 mM PMSF, and 0.2 mM phenanthroline. The sample was loaded at 1 mL/min onto a 1 mL HiTrap Q ion exchange column (Pharmacia) and eluted with a 0−210 mM KCl gradient. Due to differences in expression and affinity for the Ni-NTA between our S1 and the one used by Manstein and Hunt (1995), this additional column was required to achieve greater than 95% purity. Samples were concentrated in a Centricon-30 concentrator (Amicon), and the buffer was exchanged to 25 mM HEPES, pH 7.4, 25 mM KCl, and 1 mM DTT. Typical yields were 2 mg of S1 from 50 g of cells expressing pTIKL·S1-His, and 6 mg S1 from 25 g cells expressing pTIKL·OE·S1.

Full-length myosins were purified from *Dictyostelium* as described in Ruppel et al. (1994). Myosin was treated with bacterially expressed *Dictyostelium* myosin light chain kinase A containing the activating point mutation T166E (Smith et al., 1996). Actin was purified from chicken skeletal muscle according to the method of Pardee and Spudich (1982). The concentration of *Dictyostelium* myosin was determined by Bradford assay (Bradford, 1976) using rabbit skeletal myosin as a standard. The concentration of S1-His_6, rabbit myosin, and actin was determined spectrophotometrically, using the extinction coefficients 0.8 cm^2/mg (Ritchie et al., 1993), 0.53 cm^2/mg at 280 nm, and 0.62 cm^2/mg at 290 nm, respectively (Ruppel et al., 1994). The molecular masses of proteins were 42 kDa for actin, 130 kDa for *Dictyostelium* S1, and 500 kDa for *Dictyostelium* myosin.

ATPase Assays. We used a modification of the assay described in Ruppel et al. (1994), measuring liberated radiolabeled P_i. Buffer conditions were 25 mM imidazole, pH 7.4, 25 mM KCl, 4 mM $MgCl_2$, and 1 mM DTT. ATP concentrations varied from 12.5 μM to 3 mM for measuring the K_m for ATP. When measuring actin activation, the concentration of ATP was 3 mM. The ATP included roughly 1 nCi/μL [γ-^{32}P]ATP. Typical protein concentrations were 0.4−1.5 μM S1 with 0−75 μM actin in a volume of 50 μL. Reactions were started by adding ATP and stopped at four time points by mixing 9 μL of the reaction with 1 μL of 20% SDS and heating at 55 °C for 10 min to denature the protein. To determine the amount of [^{32}P]P_i liberated, 2 μL were spotted onto a PEI-cellulose thin layer chromatography (TLC) plate (EM Separations Technology). The TLC was run in 1.0 M formic acid, 0.4 M LiCl, and 50 mM $NaPO_4$ to separate ATP from P_i [based on Crooke et al. (1994)]. Quantification was done by measuring the ratio of free [^{32}P]-P_i to total ^{32}P using a PhosphorImager 400 S (Molecular Dynamics).

Observed rates were corrected for ATP hydrolysis by actin and the Mg^{2+}ATPase of S1 in the absence of actin. V_{max}/K_m was determined by taking the slope of a line fit to the linear phase of the ATPase rate vs concentration of actin.

When appropriate, the entire set of data was fit to the Michaelis−Menten equation. All curve fitting was done using KaleidaGraph 3.0 (Abelbeck Software).

Surface ATPase assays, used to measure the actin activation of myosin monomers, were done under the same buffer conditions as solution ATPase assays. A fixed amount of soluble myosin (in 200 mM KCl) was allowed to bind to a nitrocellulose coated cover-slip in a 1.8 cm^2 flow-cell, then washed with assay buffer containing 1 mg/mL BSA. To some samples, actin was then flowed in and allowed to bind to the myosin before being washed out with assay buffer. The reaction was started by flowing in buffer with 3 mM ATP (including 1 nCi/μL [γ-^{32}P]ATP) and 0.8% methyl cellulose and incubating at 30 °C for various times. The reaction was stopped by washing the flow-cell with an excess of stop buffer and collecting the flow-through. Free P_i was precipitated and counted in a scintillation counter as described by Ruppel et al. (1994).

Fluorescence Assays. All fluorimetry assays were performed on an AMINCO-Bowman Series 2 fluorimeter (SLM-AMINCO). The K_d of S1 for actin in the absence of ATP was measured with pyrene actin. Actin was labeled with *N*-(1-pyrene)iodoacetamide (Molecular Probes) as described in Criddle et al. (1985) and stabilized with phalloidin. Assays were performed in 25 mM HEPES, pH 7.4, 100 mM KCl, 2 mM $MgCl_2$, and 1 mM DTT at 25 or 13 °C. Pyrene actin (0.5 μM) was titrated with varied concentrations of S1-His_6. The excitation and emission wavelengths were 365 and 407 nm, respectively. Data was fit to the equation $(F_{obs} - F_0) = ((A_T + S_T + K_d) - ((A_T + S_T + K_d)^2 - 4A_TS_T)^{0.5})\text{-}(F_{obs} - F_\infty)(2A_T)^{-1}$, where A_T and S_T are the concentrations of actin and S1, respectively, and F_0 and F_{obs} are the initial and observed fluorescence values, solving for K_d and F_∞, the final level of fluorescence quenching when all the actin is bound to myosin (Criddle et al., 1985).

Cosedimentation Assay. The affinity of S1 for actin in the presence of ATP was measured using cosedimentation assays essentially as described in DasGupta and Reisler (1992). Phalloidin-stabilized actin (3 μM) and S1 at concentrations of 1.5−21 μM were mixed in the same buffer used in the ATPases (25 mM imidazole, pH 7.4, 25 mM KCl, 4 mM $MgCl_2$, and 1 mM DTT) and incubated at 22 °C for 10 min before adding 3 mM ATP and immediately spinning at 200000*g* for 10 min in a Beckman TL-100 ultracentrifuge. Pellets were resuspended in the original volume of assay buffer, and the concentration of S1 was determined by scanning Coomassie Blue stained gels with an IS-1000 Digital Imaging System (Alpha Innotech Corp.), comparing the density of bands with known standards.

Motility Assay. In vitro motility of full-length myosin, which had been treated with myosin light chain kinase, was measured by sliding filament assay using standard methods (Uyeda et al., 1990). Myosin was briefly centrifuged under solubilizing conditions in the presence of 3 μM actin and 2 mM MgATP prior to assaying to precipitate heads that bound irreversibly to actin. Solutions of 0.8 mg/mL myosin were incubated in a flow-cell for 2 min before blocking with BSA. Assay buffer conditions were 25 mM imidazole, 25 mM KCl, 4 mM $MgCl_2$, 3 mM ATP, and 0.8% methyl cellulose, with an oxygen scavenging system. Motility was measured at 30 °C.

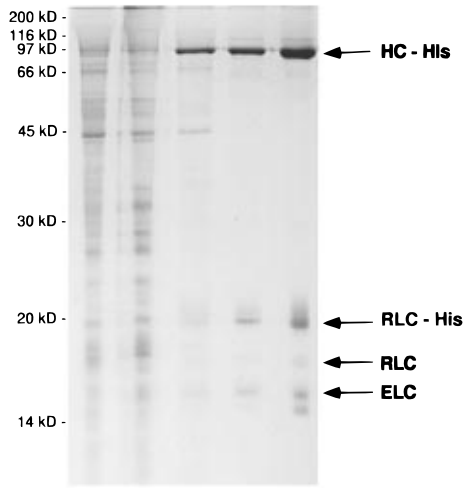

FIGURE 2: Purification of S1-His_6. Fifteen percent SDS−PAGE of samples from a typical S1 preparation from cells expressing pTIKL S1-OE, stained with Coomassie brilliant blue. Lane 1, whole-cell lysate; lane 2, second high-speed pellet; lane 3, ATP-extracted supernatant; lane 4, pool of fractions from Ni-NTA column; lane 5, pool of fractions from HiTrap Q column. Positions of molecular weight markers are shown on left, and positions of myosin heavy chain (HC), regulatory light chain (upper band with and lower band without histidine tag) (RLC), and essential light chain (ELC) on right.

RESULTS

Purification of Active Mutants as S1. The three myosins with mutations in their actin binding sites, E531Q, P536R, and R562L, had been isolated in a selection for cold-sensitive myosins that required that myosin function was rapidly regained when cells were moved from the nonpermissive temperature of 13 °C to the permissive 26 °C (Patterson & Spudich, 1996). This ensured that even at 13 °C the myosin was stable in vivo, and so loss of activity was not due to denaturation of the protein. For this reason, we believed that it should be possible to purify these proteins at 4 °C without causing irreversible damage. This was supported by the observation that all purified mutants had an activity that was stable when the proteins were stored on ice for several days or longer.

The purification of S1-His_6 forms of the cold-sensitive myosins containing the actin binding mutations is described in Materials and Methods and is shown in Figure 2. All three mutants were isolated through a purification procedure that required myosin function in the form of actin binding and ATP-dependent release, demonstrating that they retain these properties even at 4 °C. The majority of S1, both wild-type and mutant, pelleted with actin in the absence of ATP and was found in the soluble fraction after extraction with ATP. Further purification by affinity chromatography produced a sample of greater than 95% homogeneity. Because the yields of the preparations were similar between the mutant and wild-type S1s, we conclude that the mutants do not behave significantly differently from wild-type S1 in this purification.

ATP Hydrolysis Rates of S1. Solution ATPases were used to characterize the overall activity of the motors. The S1 fragment was used rather than full-length myosin because of the insolubility of myosin (due to filament formation) under the experimental conditions necessary for ATPase measurements. We were interested in determining how the mutants differ from wild-type myosin in their ability to hydrolyze ATP, to retain the products of hydrolysis in the

Table 1: ATPase Rates of S1

	basal $k_{cat} \pm$ sd (s^{-1})			actin activation $V_{max}/K_m \pm$ sd (s^{-1} mM^{-1} actin)		
	30 °C	20 °C	13 °C	30 °C	20 °C	13 °C
wild-type	0.17 ± 0.04	0.06 ± 0.01	0.05 ± 0.01	28 ± 4	8.6 ± 0.4	3.6 ± 0.4
E531Q	0.14 ± 0.02	0.08 ± 0.01	0.057 ± 0.004	1.2 ± 0.2	0.2 ± 0.1	0.0 ± 0.1
% WT	87	140	110	4	2	0
P536R	0.14 ± 0.03	0.08 ± 0.0	0.06 ± 0.02	4.5 ± 0.3	1.6 ± 0.1	0.60 ± 0.07
% WT	84	130	120	16	19	17
R562L	0.16 ± 0.05	0.06 ± .01	0.052 ± 0.005	7.6 ± 0.7	1.0 ± 0.1	0.49 ± 0.06
% WT	94	110	100	27	12	14

Table 2: Apparent Affinity of S1s for ATP

	K_m (μM ATP)
wild-type	32 ± 7
E531Q	22 ± 7
P536R	29 ± 8
R562L	36 ± 10

absence of actin, and to accelerate the release of products in the presence of actin. These are important characteristics of the standard motor and thus useful parameters for describing the effects of the various mutations. This assay was performed at 30, 20, and 13 °C to examine whether the mutant myosins exhibit in vitro the cold sensitivity observed in vivo.

The mutations E531Q, P536R, and R562L did not significantly change the Mg^{2+}ATPase of S1 in the absence of actin at any temperature assayed (Table 1). Therefore, the release of P_i in the absence of actin, which is the rate-limiting step of the basal ATPase rate, is not greatly affected in these mutants.

We also measured the apparent affinity for ATP in the absence of actin, and found no significant difference between any of the three mutants and wild-type. The K_m for ATP is approximately 30 μM ATP at 30 °C for the wild-type and all three mutant S1s (Table 2). We interpret the lack of significant changes in the K_m for ATP and the steady state hydrolysis rate in the absence of actin as good indications that these point mutations do not greatly affect the actin-independent activities of the enzyme.

In contrast to their basal activities, the actin activation of all of the mutants is greatly reduced compared to wild-type (Figure 3 and Table 1). The slope of the linear portion of the data was used to calculate the apparent second-order rate constant V_{max}/K_m, also known as the catalytic efficiency of the reaction. The V_{max}/K_m of wild-type S1 was determined to be 28 s^{-1} mM^{-1} actin at 30 °C. The activation by actin of the mutants' ATPase rates was significantly reduced and ranges from nearly 30% (8 s^{-1} mM^{-1}) of the wild-type rate for R562L S1 to just 1.2 s^{-1} mM^{-1} or 4% of wild-type for E531Q S1. While the ATPase activation dropped with lower temperatures for all S1s, the actin activation of P536R S1 changed roughly proportionally to wild-type with temperature, while R562L S1 became relatively more defective at lower temperature. While the activation was 27% that of wild-type at 30 °C, it dropped to 14% at 13 °C. Thus, there are apparent cold-sensitive defects in vitro as well as in vivo for the R562L mutant. Although we do not believe that the behavior of E531Q S1 is necessarily cold sensitive, being very low at all temperatures, it is interesting to note that we could detect no activation by actin of this mutant at 13 °C.

In most cases, the K_m for actin (which is a measure of the apparent affinity of myosin for actin in its weak-binding state) was too great to determine K_m and V_{max} independently under the conditions used. At 30 °C, we were able to make rough estimates of V_{max} for the R562L and wild-type S1s. When the full data set of the actin-activated ATPase of wild-type and R562L S1s were fit to the Michaelis−Menten equation, the predicted V_{max} for wild-type was 2.4 ± 0.3 s^{-1} and R562L was 0.6 ± 0.2 s^{-1}. Due to the fact that none of the data was taken well above the K_m for actin, these rates should be viewed with some skepticism; however, we feel that the change observed in V_{max} for R562L S1 is significant.

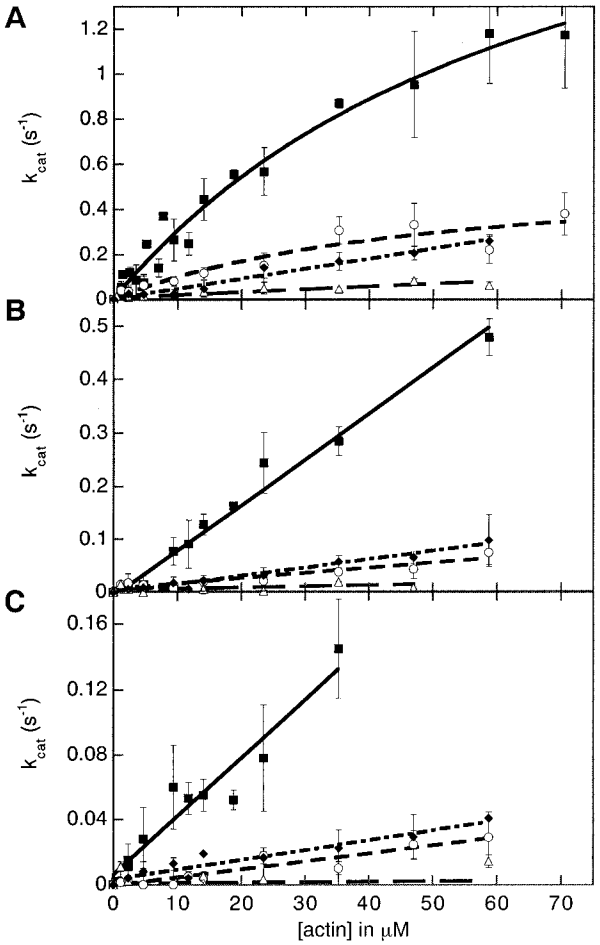

FIGURE 3: Actin activation of Mg^{2+} ATPase of S1. The rates of ATP hydrolysis were measured at (A) 30 °C, (B) 20 °C, and (C) 13 °C and corrected for basal ATPase rates under conditions described in Materials and Methods. Symbols represent wild-type *(closed squares)*, E531Q *(open triangles)*, P536R *(closed diamonds)*, and R562L *(open circles)*. Error bars show the standard deviation of the data. Straight lines were fit to the initial slopes to define V_{max}/K_m. (Values are shown in Table 1.) For wild-type and R562L at 30 °C (panel A), curves are fit to the entire data set using the Michaelis−Menton equation. V_{max} = 2.4 ± 0.3 and 0.6 ± 0.2 s^{-1}; K_m = 70 ± 20 and 50 ± 30 μM actin for wild-type and R562L S1, respectively.

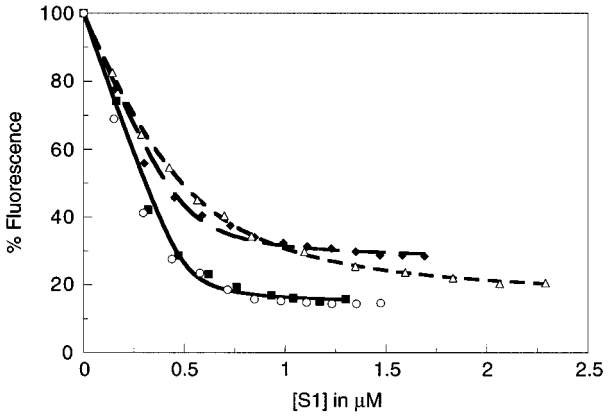

FIGURE 4: Titration of pyrene actin with mutant S1s. The change in fluorescence from 0.5 μM pyrene-labeled actin with increasing amounts of S1 is shown. Titrations were performed at 25 °C. Symbols represent wild-type *(closed squares)*, E531Q *(open triangles)*, P536R *(closed diamonds)*, R562L *(open circles)*, and error bars show the standard deviation of data. The curves shown are fit to wild-type, E531Q, and P536R as described in Materials and Methods to determine the K_d and the extent of quenching with saturated binding. K_d = 11, 140, 30, and 8 nM, and the fluorescence was quenched down to 14 ± 2, 14 ± 1, 27 ± 1, and 13 ± 2% of the initial fluorescence for the wild-type, E531Q, P536R, and R562L S1s, respectively.

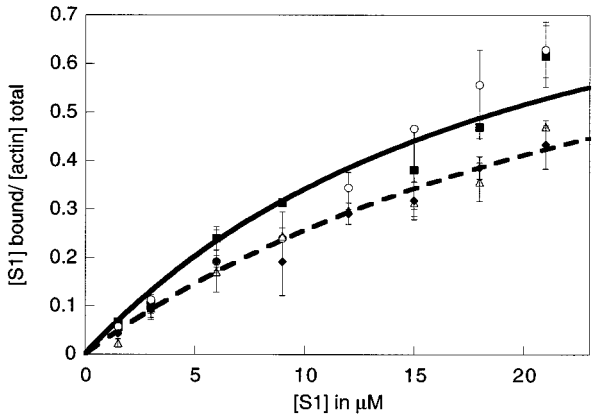

FIGURE 5: Cosedimentation of S1 with actin in the presence of ATP. The amount of S1 that pelleted with 3 μM actin in the presence of 3 mM Mg^{2+}ATP was determined by densitometry of Coomassie Blue stained gels as described in Materials and Methods. Symbols represent wild-type *(closed squares)*, E531Q *(open triangles)*, P536R *(closed diamonds)*, and R562L *(open circles)*, and error bars show the standard deviation of data. The curves shown are the best fits to the data for wild-type (solid line) and E531Q (dashed line). The K_d was determined to be 17 ± 2, 27 ± 1, 28 ± 1 , and 17 ± 2 μM for wild-type, E531Q, P536R, and R562L S1, respectively.

Actin Binding Affinity of Mutant S1s. In order to address the possibility that the low levels of actin activation of the mutants' ATPase rates were due to low affinity of the S1s for actin, we compared the dissociation constants, K_d, of the wild-type and mutant S1s in the absence of nucleotide, using pyrene-labeled actin at 25 °C (Figure 4). The affinity of R562L S1 for actin is not significantly different from that of the wild-type. There is a small increase in the estimated K_d of P536R S1 to 30 nM. However, this may not be significantly different from the wild-type. By comparing the best fits of the data to models of different affinities, we estimate that the error is such that the dissociation constants of wild-type and R562L S1s are between 5 and 25 nM, while that of the P536R mutant is 20−40 nM. More notably, P536R S1 has a large change in the total quenching of the pyrene label at saturation, which is 30% of the fluorescence of pyrene−actin alone, compared to roughly 15% seen for wild-type and the other mutants. This indicates that the interaction between the bound myosin head and the pyrene is somehow perturbed in this mutant. The mutation E531Q has caused a large change in affinity for actin in the absence of nucleotide, so that the K_d is now between 120 and 170 nM. Thus, the mutations in the actin binding site have very different effects on rigor binding. We also measured the K_d of the myosin fragments at 13 °C and saw no significant change from that observed at 25 °C (data not shown).

We examined the affinity of the S1s in the presence of ATP using cosedimentation assays (Figure 5). By using densitometry to determine the amount of S1 bound to 3 μM actin at a range of S1 concentrations (total) from 1.5 to 21 μM, we found that the K_d for actin interacting with wild-type S1 is 17 μM. This is about 1000-fold weaker than the interaction in the absence of nucleotide. The affinities of the mutants for actin were 27, 28, and 17 μM for E531Q, P536R, and R562L S1s, respectively. Thus, the affinity of the mutant S1s for actin in the presence of ATP is within 2-fold that of wild-type S1. We also used cosedimentation in the absence of ATP to demonstrate that ≥95% of S1 was capable of binding actin for both the wild-type and mutant S1s.

In Vitro Motility of Mutant Myosins. The movement of actin filaments by surface-bound myosin can indicate the point in the cycle at which the myosin is defective. At high myosin concentrations, mutants that are slowed only in weakly bound states are expected to move actin at normal velocities, while those delayed in strongly bound states would move actin more slowly (Siemankowski et al., 1985). We measured the velocity of actin filaments in our standard motility assay using full-length myosins. Myosin was used rather than S1 for this experiment because of the roughly 25-fold lower velocities observed for wild-type *Dictyostelium* S1 compared to myosin (Manstein et al., 1989b), probably due to incorrect orientation of the S1 on the nitrocellulose surface in the motility assay.

No uniform movement was observed for the E531Q, P536R, or R562L myosins, although all of them bound actin in the absence of ATP. Under the same conditions, wild-type myosin moved actin at an average of 2.6 ± 0.3 μm/s. While occasional brief, unidirectional movement of a single actin filament was observed with R562L, at least 95% of filaments observed wiggled at the ends without any unidirectional movement. Strikingly, not only did P536R fail to produce movement, but there was little difference in the appearance of P536R-bound actin before and after adding ATP, even at the ends of filaments, which tend to wiggle in the presence of ATP with most forms of myosin. This suggests that P536R binds actin filaments tightly for an increased percentage of its ATPase cycle, which results in more heads tightly binding to an actin filament at any given time.

In order to better define the properties of the mutants, we also performed motility assays with equal concentrations of wild-type and mutant myosins to determine the ability of the mutants to retard actin movement driven by wild-type myosin (Figure 6). This was done under concentrations at which the wild-type myosin alone was sufficient for maximum velocity. The presence of E531Q or R562L myosin somewhat slowed the velocity of actin filaments, to approximately 75% the rate of the same amount of wild-type protein alone. P536R myosin had a much greater effect,

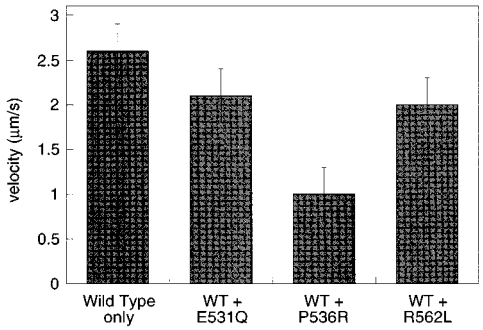

FIGURE 6: Sliding velocities of mixtures of mutant and wild-type myosins. Velocities were measured at 30 °C under the conditions described in Materials and Methods. The mean sliding velocity produced by wild-type myosin or by mixtures of equal amounts of wild-type and mutant myosins are shown. Measurements were done at protein concentrations at which the wild-type alone was sufficient for maximum velocity. Error bars show the standard deviation of velocities of smoothly moving filaments.

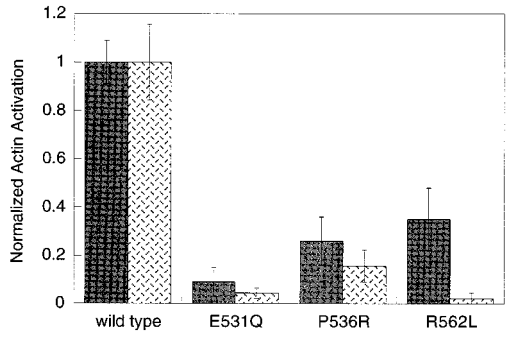

FIGURE 7: Comparison of the actin activation of S1 and myosin Mg^{2+}ATPases . The level of actin-activation above basal ATPase of S1 *(solid bars)* and full-length myosin *(stippled bars)* with 24 μM actin at 30 °C is shown. Data has been normalized between all S1s or all myosins by dividing the observed rate of activation of each mutant by the appropriate wild-type rate. Error bars show standard deviation.

slowing movement to 35% of the wild-type myosin's speed. This result is consistent with our hypothesis that P536R has increased the strongly bound state time of the myosin. We emphasize that this effect was not due to the presence of denatured protein, as just before assaying them each protein was centrifuged in the presence of actin and ATP to remove insoluble protein as well as heads that irreversibly bound to actin.

Actin Activation of Mutant Myosin ATPases. As a control for the activity of the mutant myosins, we measured their solution ATPases with or without 24 μM actin and compared them with the equivalent conditions of the ATPase assays described above for the S1 forms of the proteins (Figure 7). The ATPase rates of the myosin were quite reproducible between preparations. We observed that the full-length myosin and S1 forms of E531Q and P536R have approximately the same proportion of actin activation compared to wild-type. Surprisingly, the R562L myosin is less activated than the corresponding S1. The activities of myosin and S1 are not predicted to be necessarily identical, due to a variety of factors including the filamentous state of myosin under the low-salt conditions used, as well as the regulation of myosin (Tan et al., 1992) but not of S1 by phosphorylation of the regulatory light chain (Ikebe & Hartshorne, 1985). We expected, however, to see an increase in activity of myosin with actin roughly proportional to that seen with S1.

The low activation of R562L myosin compared to S1 is not due to a difference in the ATPase of filaments versus monomers. The activation of the ATPase rate of R562L myosin monomers was determined by attaching the myosin to a surface under solubilizing, high-salt conditions, and then assaying under low salt ATPase buffer conditions. Under conditions at which wild-type myosin hydrolyzed less than 0.1 nmol of ATP/min without actin and 1.0 nmol/min with actin, an equal amount of R562L myosin hydrolyzed less than 0.1 nmol/min both with and without actin. This demonstrates that the loss of actin activation of R562L myosin, compared to that observed with R562L S1, is not due to the formation of myosin filaments.

DISCUSSION

The isolation of conditional mutations in the actin binding region of the *Dictyostelium* myosin II heavy chain by Patterson and Spudich (1996) provided us with a unique opportunity to understand why and how specific residues are important for myosin function. Our hypothesis that the myosin mutations E531Q, P536R, and R562L are defective due to loss of important interactions between actin and myosin has been supported by the data that shows that the mutants have lost certain actin-dependent functions without greatly changing the actin-independent properties of the normal motor. The data is summarized in Table 3.

These mutations neither change the apparent affinity of S1 for ATP in the absence of actin nor do they greatly perturb the basal Mg^{2+}ATPase rate at all temperatures measured. Thus, it is clear that some properties of the molecule are unaffected by these substitutions, including nucleotide binding and the tight regulation of product release.

The interactions of the mutant myosins with actin are significantly different from wild-type myosin. Although all mutants retain the ability to bind and release actin in an ATP-dependent manner, even at low temperatures, they are greatly impaired in the actin activation of their ATPase rates. Even at 30 °C, which is slightly above the in vivo permissive temperature, the mutant S1s are poorly activated by actin, with V_{max}/K_m values that range from 30 to just 4% of the wild-type. Although in the presence of ATP none of the mutations causes even a 2-fold change in the binding of S1 to actin, E531Q S1 binds actin at least 10-times more weakly than wild-type S1 in the absence of nucleotide. Thus, these experiments indicate that there are defects in the interactions of the mutant myosins with actin and that these defects are different for different mutants.

The motility assays on mixtures of equal amounts of wild-type and mutant myosins addressed the question of what points in the cycle are affected by the myosin mutations. This technique has been used to determine the load that myosin can put on actin during active cycling (Sweeney et al., 1994; Ruppel & Spudich, 1996). Since there is little if any load placed on actin by the E531Q and R562L myosins, they are probably inhibited prior to the weak-to-strong actin binding transition. Thus, like wild-type myosin, the predominantly populated intermediates are interacting only weakly with actin. In contrast, P536R myosin places significant drag on actin and thus is strongly bound to actin for a significant fraction of the cycle time.

R562. We have shown that the reduced activation of the ATPase rate of R562L S1 is correlated with a reduction in V_{max} (Figure 3). This could be caused by a normally rate-limiting step being slowed or a different step that has become rate limiting. Since the mutation at R562 does not cause

Table 3: Data Summary

		ATP hydrolysis (30 °C)		affinity for actin (K_d)		
	apparent affinity for ATP (K_m) (μM)	basal (s^{-1})	actin activation (mM^{-1} s^{-1})	−ATP (nM)	+ATP (μM)	motility of wild-type with mutant myosin (μm/s)
wild-type	32	0.17	28	11	17	2.6
E531Q	22	0.14	1.2	140	27	2.1
P536R	29	0.14	4.5	30	28	1.0
R562L	36	0.16	7.6	8	17	2.0

myosin to exert drag on sliding actin filaments, the slowed step is likely to occur when myosin is only weakly associated with actin. Thus, the reduced V_{max} is probably due to a rate change at a step that occurs before actin is strongly bound, such as the ATP hydrolysis step or the step at which an initially weak interaction between actin and myosin becomes strong, simultaneously stimulating P_i release from myosin. Because of the location in the actin binding site, we favor the model that the defect of the mutation at R562 is that it is inhibited in this P_i release step that triggers the weak-to-strong transition in actin binding, although other alternatives cannot be ruled out without further kinetic analysis.

As discussed above, the docking of the S1 and actin crystal structures led us to postulate that there may be an interaction between R562 and the actin-charged pair E99/E100. As demonstrated by analysis of the actin mutant E99A/E100A by Miller and Reisler (1995), this pair of residues is important for weak interactions between actin and myosin and may also contribute to myosin's actin-activated ATPase rate. Our data for R562L are not consistent with this data, as we see no change in the affinity for actin in the presence of ATP with this mutant. Therefore, we conclude that the R562 residue of myosin is not interacting directly with the actin E99/E100 charged pair.

The reason for the observed differences in the actin activation of ATP hydrolysis between the S1 and myosin forms of R562L is not clear (Figure 7). By comparing the actin activation of surface-bound monomeric R562L myosin to the wild-type, we have eliminated the possibility that the differences in R562L myosin from S1 arise from the formation of bipolar thick filaments by myosin. Another potential explanation is that the full-length myosin form, unlike S1, is regulated by light chain phosphorylation and so the myosin could be affected by both the change in the rate-limiting step discussed above and a change in regulation. Myosin's 50/20 kDa loop, which lies in the actin binding site, has been shown to play a role in regulation. Chimeras of loops from unregulated myosins placed in the regulated smooth muscle heavy meromyosin fragment have been shown to be more actin-activated when the regulatory light chain is unphosphorylated than the wild-type (Rovner et al., 1995). Thus, changes in myosin's actin binding site can affect the regulation of actin activation. In the case of the mutation at R562, there appears to be the opposite effect, so that the full-length myosin may be "hyper-regulated". In *Dictyostelium* myosin, certain regions of the tail have been shown to be required for regulation (Liu et al., 1996). Taken together, it seems possible that a direct interaction of the actin binding site with the tail is required for regulation and that this interaction may be strengthened by the mutation R562L.

E531. The mutant E531Q myosin has almost no actin activation of its ATPase activity. The observed decrease in affinity of S1 for actin in the absence of ATP, with only a small decrease in the affinity in the presence of ATP, suggests that the residue E531 is more important for the strong binding interactions than the weak. We suggest that this could also account for the poor actin activation observed in the ATPase assays, if the contact were important at the weak-to-strong actin binding transition as well as at the end of the stroke (the rigor interaction). The low activation of the ATPase activity by actin might then be due entirely to a decrease in the V_{max}, although our data does not rule out an increase in K_m. Our model is that E531 may be forming a salt bridge with an actin residue throughout the strongly bound state.

P536. The defects of P536R myosin are strikingly different from those observed for the mutations of R562 and E531. Surface-bound P536R myosin holds actin filaments firmly in the presence of ATP, inhibiting Brownian motion of the actin filaments. It also significantly slows actin filaments that are being moved in sliding assays by wild-type myosin. Such effects suggest that P536R myosin has either a longer than normal strongly bound state time or an increase in the affinity of myosin for actin in the weakly bound state. However, the increase in the affinity for actin in the weak-binding state was ruled out by the cosedimentation assays performed in the presence of ATP, which showed that the K_d for actin is slightly increased from that of wild-type S1 under these conditions. Thus, we believe that when P536R myosin heads do become strongly bound to actin, they spend an unusually long time in this state. This could be due to a failure to release ADP, which would prevent the rebinding of ATP and the release of the myosin head from actin. Alternatively, it could result from a significant stabilization of an interaction between actin and myosin during the stroke. Such a strengthened interaction would be an especially exciting result as it does not appear in rigor binding affinity (Figure 4) and would argue that there are interactions that are important in a strong binding interaction that occurs during the stroke, but not in rigor.

Role of Myosin in Vivo. Comparison of the effects of these mutations in vivo, observed by Patterson and Spudich (1995, 1996), and the in vitro results described here suggests a few things about the requirements for myosin activity in the cell. First of all, it appears that levels of activity far below wild-type levels are sufficient for the myosin-requiring azide response in *Dictyostelium*. Cells were assayed for myosin function by determining their response to azide, which causes cells with active myosin to round up and lose their attachment to the substratum on which they are migrating. Cells lacking myosin fail to undergo this response. P536R myosin, for which we observed no motor activity, was shown to respond to azide far better than cells completely lacking myosin, although less well than the other two mutants that do not greatly impede actin sliding (Patterson & Spudich, 1996). Differences between the conditions in vivo and in vitro, including the potential for the colocalization of actin and

myosin to high concentrations, may be a large factor in the ability of all of these mutant myosins to at least partially function in vivo. The cold sensitivity observed in vivo has been correlated to a cold sensitivity in vitro for R562L myosin, but P536R myosin shows no indication of being any more affected by temperature than wild-type myosin. Thus, the in vivo phenotype for P536R myosin suggests that there may be a temperature-dependent threshold, so that low levels of myosin activity may be sufficient at higher temperatures and not at lower ones.

It is also interesting to consider that the azide response is relatively sensitive to the presence of any myosin function. Thus, cells that respond as myosin-plus in this assay may appear "minus" in other in vivo assays that are used to determine the presence of myosin function, including growth in suspension (Giese, K. C., & Spudich, J. A., unpublished observation) and *Dictyostelium* development (Patterson & Spudich, 1995). Therefore, it is possible that even at the permissive temperature, some of these mutants may have only very low amounts of motor activity in vivo.

The specific goal of this study is to understand the effect of phenotypically selected mutations of the *Dictyostelium* myosin that lie in myosin's actin binding site on its activity and in doing so learn about the important contacts that occur in this dynamic system. The effects of the mutations at the residues E531, P536, and R562 are varied, illustrating the different types of interactions between myosin and actin that can be changed. The changes at these positions have affected various characteristics of the motor, including the length of the strongly bound state time, the maximum rate of the actin-activated ATPase, and the binding affinity of myosin for actin. Thus, these residues have distinct functions that help define the structure−function map of the interactions between actin and myosin.

ACKNOWLEDGMENT

We thank Taro Uyeda for generously sharing the *Dictyostelium* expression plasmids with us before their publication and Ken Holmes and Michael Lorenz for providing the coordinates for the structure figure. We also thank Emil Reisler, Dietmar Manstein, Bruce Patterson, Geeta Narlikar, Steffen Nock, and Coleen Murphy for helpful comments on the work and the manuscript.

REFERENCES

Bradford, M. M. (1976) *Anal. Biochem. 72*, 248−254.
Cook, K. R., Root, D., Miller, C., Reisler, E., & Rubenstein, P. A. (1993) *J. Biol. Chem. 268*, 2410−2415.
Criddle, A. H., Geeves, M. A., & Jeffries, T. (1985) *Biochem. J. 232*, 343−349.
Crooke, E., Akiyama, M., Rao, N., & Kornberg, A. (1994) *J. Biol. Chem. 269*, 6290−6295.
DasGupta, G., & Reisler, E. (1992) *Biochemistry 31*, 1836−1841.
Egelhoff, T. T., Titus, M. A., Manstein, D. J., Ruppel, K. M., & Spudich, J. A. (1991) *Methods Enzymol. 196*, 319−34.
Geeves, M. A. (1991) *Biochem. J. 274*, 1−14.
Goldman, Y. E. (1987) *Annu. Rev. Physiol. 49*, 637−654.
Holmes, K. C., Popp, D., Gebhard, W., & Kabsch, W. (1990) *Nature 347*, 44−49.
Huxley, A. F., & Simmons, R. M. (1971) *Nature 233*, 533−538.
Huxley, H. E. (1969) *Science 164*, 1356−1366.
Ikebe, M., & Hartshorne, D. J. (1985) *Biochemistry 24*, 2380−2387.
Johara, M., Toyoshima, Y. Y., Ishijima, A., Kojima, H., Yanagida, T., & Sutoh, K. (1993) *Proc. Natl. Acad. Sci. U.S.A. 90*, 2127−2121.
Kraulis, P. J. (1991) *J. Appl. Crystallogr. 24*, 946−950.
Liu, X., Ito, K., Lee, R. J., & Uyeda, T. Q. P. (1996) *Mol. Biol. Cell 7*, 34a.
Lymn, R. W., & Taylor, E. W. (1971) *Biochemistry 10*, 4617−4624.
Manstein, D. J., & Hunt, D. M. (1995) *J. Muscle Res. Cell Motil. 16*, 325−332.
Manstein, D. J., Ruppel, K. M., & Spudich, J. A. (1989a) *Science 246*, 656−8.
Manstein, D. J., Titus, M. A., De Lozanne, A., & Spudich, J. A. (1989b) *EMBO J. 8*, 923−932.
Miller, C. J., & Reisler, E. (1995) *Biochemistry 34*, 2694−2700.
Miller, C. J., Doyle, T. C., Bobkova, E., Botstein, D., & Reisler, E. (1996) *Biochemistry 35*, 3670−3676.
Pardee, J. D., & Spudich, J. A. (1982) *Methods Cell Biol. 24*, 271−289.
Patterson, B., & Spudich, J. A. (1995) *Genetics 140*, 505−515.
Patterson, B., & Spudich, J. A. (1996) *Genetics 143*, 801−810.
Rayment, I., Holden, H. M., Whittaker, M., Yohn, C. B., Lorenz, M., Holmes, K. C., & Milligan, R. A. (1993a) *Science 261*, 58−65.
Rayment, I., Rypniewski, W., Schmidt-Base, K., Smith, R., Tomchick, D., Benning, M., Winkelmann, D., Wesenberg, G., & Holden, H. (1993b) *Science 261*, 50−58.
Ritchie, M. D., Geeves, M. A., Woodward, S. K. A., & Manstein, D. J. (1993) *Proc. Natl. Acad. Sci. U.S.A. 90*, 8619−8623.
Rovner, A. S., Freyzon, Y., & Trybus, K. M. (1995) *J. Biol. Chem. 270*, 30260−30263.
Ruppel, K. M., & Spudich, J. A. (1996) *Mol. Bio. Cell 7*, 1123−1136.
Ruppel, K. M., Uyeda, T. Q.-P., & Spudich, J. A. (1994) *J. Biol. Chem. 269*, 18773−18780.
Sambrook, J., Fritsch, E. F., & Maniatis, T. (1989) *Molecular Cloning. A Laboratory Manual*, 2nd ed., Cold Spring Harbor Laboratory Press, Plainview, NY.
Schröder, R. R., Manstein, D. J., Jahn, W., Holden, H., Rayment, I., Holmes, K. C., & Spudich, J. A. (1993) *Nature 364*, 171−174.
Sellers, J. R., & Goodson, H. V. (1995) in *Protein Profiles* (Sheterline, P., Ed.) pp 1323−1423, Academic Press Limited, London.
Siemankowski, R. F., Wiseman, M. O., & White, H. D. (1985) *Proc. Natl. Acad. Sci. U.S.A. 82*, 658−662.
Smith, J. L., Silveira, L. A., & Spudich, J. A. (1996) *EMBO J. 15*, 6075−6083.
Sussman, M. (1987) in *Dictyostelium discoideum: Molecular approaches to Cell Biology* (Spudich, J. A., Ed.) pp 9−29, Academic Press, Orlando.
Sutoh, K., Ando, M., Sutoh, K., & Toyoshima, Y. Y. (1991) *Proc. Natl. Acad. Sci. U.S.A. 88*, 7711−7714.
Sweeney, H. L., Straceski, A. J., Leinwand, L. A., Tikunov, B. A., & Faust, L. (1994) *J. Biol. Chem. 269*, 1603−1605.
Tan, J. L., Ravid, S., & Spudich, J. A. (1992) *Annu. Rev. Biochem. 61*, 721−759.
Uyeda, T. Q. P., Kron, S. J., & Spudich, J. A. (1990) *J. Mol. Biol. 214*, 699−710.
Uyeda, T. Q.-P., Ruppel, K. M., & Spudich, J. A. (1994) *Nature 368*, 567−569.
Uyeda, T. P. Q., Abramson, P. D., & Spudich, J. A. (1996) *Proc. Natl. Acad. Sci. U.S.A. 93*, 4459−4464.
Whittaker, M., Wilson-Kubalek, E. M., Smith, J. E., Faust, L., Milligan, R. A., & Sweeney, H. L. (1995) *Nature 378*, 748−751.
Yamamoto, K. (1990) *Biochemistry 29*, 844−848.
Yamamoto, K. (1991) *J. Mol. Biol. 217*, 229−233.

BI963141F